Biogeosciences
Discussions

Historical reconstruction of ocean acidification in the Australian region

A. Lenton[1], B. Tilbrook[1,2], R. J. Matear[1], T. Sasse[3], and Y. Nojiri[4]

[1]Oceans and Atmosphere Flagship, Hobart, Australia
[2]Antarctic Climate and Ecosystems Co-operative Research Centre, Hobart, Australia
[3]Climate Change Research Centre, Kensington Campus, University of New South Wales, Sydney, Australia
[4]National Institute for Environmental Studies, Tsukuba, Japan

Correspondence to: A. Lenton (andrew.lenton@csiro.au)

Abstract

The increase in atmospheric greenhouse gases over the last 200 years has caused an increase in ocean acidity levels. Documenting how the ocean has changed is critical for assessing how these changes could impact marine ecosystems and for the management of marine resources. We use present day ocean carbon observations from shelf and offshore waters around Australia, combined with neural network mapping of CO_2, to estimate the current seasonal and regional distributions of carbonate chemistry (pH and aragonite saturation state). These predicted changes in carbonate chemistry are combined with atmospheric CO_2 concentration ~~changes since~~ to reconstruct pH and aragonite saturation state changes over the last 140 years (1870–2013). The comparison with data collected at Integrated Marine Observing System National Reference Station sites located on the shelf around Australia shows both the mean state and seasonality for the present day is well represented by our reconstruction, with the exception of sites such as the Great Barrier Reef. Our reconstruction predicts that since 1870 an average decrease in aragonite saturation state of 0.48 and of 0.09 in pH has occurred in response to increasing oceanic uptake of atmospheric CO_2. Our reconstruction shows that seasonality is the dominant mode of variability, with only small interannual variability present. Large seasonal variability in pH and aragonite saturation state occur in Southwestern Australia driven by ocean dynamics (mixing) and in the Tasman Sea by seasonal warming (in the case of aragonite saturation state). The seasonal and historical changes in aragonite saturation state and pH have different spatial patterns and suggest that the biological responses to ocean acidification are likely to be non-uniform depending on the relative sensitivity of organisms to shifts in pH and saturation state. This new historical reconstruction provides an important to link to biological observations to help elucidate the consequences of ocean acidification.

1 Introduction

The ocean plays a key role in reducing the rate of global climate change, absorbing approximately 30 % of the anthropogenic CO_2 emitted over the last 200 years (Ciais et al., 2013), and more than 25 % of current CO_2 emissions (Le Quéré, 2015). The CO_2 taken up by the ocean reacts in seawater, leading to decreases in pH and dissolved carbonate ion concentrations (CO_3^{2-}), these changes being collectively referred to as ocean acidification. Over the past 200 years, it is estimated that there has been a 0.1 unit reduction in the ocean's surface pH, or 26 % increase in the concentration of hydrogen ion concentrations in seawater (Doney et al., 2009).

Current projections suggest that the increase in hydrogen ion concentration is likely to greater than 100 % (than the preindustrial period) by the end of the century under high emissions trajectories e.g. Matear and Lenton (2014). Furthermore these changes will persistent for many millennia e.g. Frolicher and Joos (2010). Ocean acidification is likely to impact the entire marine ecosystem – from microbial communities to top predators. Factors that can be impacted include reproductive health, organism growth and physiology, species composition and distributions, food web structure and nutrient availability (Aze et al., 2014; Doney et al., 2012; Dore et al., 2009; Fabry et al., 2008; Iglesias-Rodriguez et al., 2008; Munday et al., 2010, 2009).

Aragonite is a metastable form of calcium carbonate that is produced by major calcifiers in coral reef ecosystems, including reef building coral, and is the predominant biogenic carbonate mineral in warm and shallow waters of the tropics (Stanley and Hardie, 1998). The aragonite saturation state of seawater has been used as a proxy for estimating net calcification rates for corals e.g. Langdon and Atkinson (2005). Projections suggest that by as early as 2050 growth rates of reef building coral may slow to such levels that coral reefs may start to dissolve (Silverman et al., 2009). The impact of acidification combined with other stresses, such as ocean warming, has implications for the health, longer-term sustainability and biodiversity of reef ecosystems (Doney et al., 2012; Dore et al., 2009).

The impact of these changes on the marine environment is fundamental for the management of future marine resources, for nations like Australia with its extensive coastline and regions of international significance such as the Great Barrier Reef. An historical record of the changes that have occurred since the preindustrial period allows us to (i) correctly attribute observed responses over the historical period; (ii) assess how well climate models represent spatial patterns of ocean acidification for the period that overlaps observations (e.g. IPCC AR5); (iii) quantify the magnitude of seasonal and interannual variability, and identify the drivers of this variability; and (iv) provide important boundary conditions for regional high resolution regional models.

Despite potential impacts of ocean acidification for the Australian region, the number of carbonate chemistry measurements is sparse. The few datasets collected only characterise variability and the mean state in specific environments e.g. (Shaw et al., 2012; Albright et al., 2013) or attempt to synthesize these into regional or habitat-based studies e.g. Gagliano et al. (2010). The only seasonally-resolved observational dataset available to characterize the mean state around Australia in the present day is Takahashi et al. (2014), but this data has coarse resolution and only focuses on the open ocean areas. Studies that have reconstructed the longer-term variability of ocean acidification from coral proxies have been of regional scale and are temporally coarse e.g. Pelejero et al. (2005) and Calvo et al. (2007).

The goals of our study are: (i) reconstruct the observed variability and mean state in pH and aragonite saturation state in the present day around Australia at high spatial resolution and (ii) reconstruct the changes that have occurred in the Australian region over the last 140 years (1870–2013). To this end, we first develop a new salinity–alkalinity relationship for Australian waters based on observations collected around Australia over the last two decades. We then assess our reconstructed pH and aragonite saturation state fields with data collected around Australia at the Integrated Marine Observing System National Reference Stations (IMOS-NRS) sites. Finally, we present the reconstructed aragonite saturation state and pH in the Australian region and discuss the seasonal, interannual and long-term changes in these fields. The re-

constructed fields as well as the calcite saturation state, dissolved inorganic carbon dioxide (DIC), total alkalinity (ALK), sea surface temperature and salinity are all available online at http://imos.aodn.org.au.

2 Methods

In this study we focus on the Australian region (Fig. 1) delineated nominally by the Subtropical Front (50° S) in the south and the equator (0°) in the north, and between 95–170° E. This region encompasses part of the eastern Indian Ocean and Indonesian Seas and a large part of the Tasman and Coral Seas. The seasonal cycle of physical, chemical, and biological properties of the surface ocean mixed layer this region are described in Condie and Dunn (2006), and will not be described further in this paper. The characterization of the ~~carbon~~ system requires two of six potential carbon parameters (i.e. pH, total dissolved inorganic carbon, total alkalinity, partial pressure of carbon dioxide, bicarbonate, carbonate), from which all the parameters of the ocean carbon system can be calculated. We first use $p\text{CO}_2$ and total alkalinity to reconstruct the changes in ocean acidification.

The oceanic values of $p\text{CO}_2$ were taken from an updated version of (Sasse et al., 2013) climatology that used a neural network to map values around Australia on a 1° × 1° degree grid each month for the year 2000. These $p\text{CO}_2$ values provide significantly higher spatial data coverage than the global climatology of Takahashi et al. (2009).

To extend the oceanic $p\text{CO}_2$ values into the past and the future, the value of $\Delta p\text{CO}_2$ ($p\text{CO}_{2\text{air}} - p\text{CO}_{2\text{sea}}$) was first calculated using Sasse et al. (2013) for the year 2000. This $\Delta p\text{CO}_2$ value was then ~~transformed into~~ a time series of oceanic $p\text{CO}_2$ between 1870 to 2013, by adding this to the observed atmospheric CO_2 ~~value~~ over this period using the atmospheric history constructed by Le Quéré et al. (2015).

As only very few measurements of total alkalinity (ALK) exist in the Australian region e.g. GLODAP (Key et al., 2004), we use the relationship between ALK and salinity to estimate ALK in the Australian region. While many studies have quantified this rela-

tionship globally e.g. Takahashi et al. (2014) and Lee et al. (2006) and regionally e.g. Kuchinke et al. (2014), to date no specific relationship has been developed for the entire Australian region.

To develop this relationship ~~a series of~~ concomitant measurements of salinity and alkalinity (Table 1; Fig. 1) ~~taken over several years from around Australia~~, from ships transects and some of the IMOS (NRS) (Lynch et al., 2014) ~~were used~~. We determined the relationship to be:

$$\text{ALK}(\mu\text{mol}\,\text{kg}^{-1}) = (2295.9 \pm 0.1) + (64.4 \pm 0.3) \times (\text{SAL} - 35.0) \tag{1}$$

This relationship is based on a type 2 linear regression, accounting for uncertainty in both ~~the~~ salinity and ALK measurements ~~of~~ 0.05 and 3 $\mu\text{mol}\,\text{kg}^{-1}$ respectively. This new relationship was applied to the climatology of salinity (0.5° × 0.5°/daily) taken from the CSIRO Atlas of Regional Seas 2012 (CARS; Ridgway et al., 2002) as no long-term high spatial and temporal resolution observations of ocean surface salinity at present exist around Australia (nor globally). Nevertheless, based on sparse measurements Durack and Wijffels (2010) suggested that there has been amplification of the global hydrological cycle that has resulted in surface salinity changes over the last 50 years. Their estimated changes around Australia are not uniform and are typically less than ±0.1, which introduces only a 6.4 $\mu\text{mol}\,\text{kg}^{-1}$ change in ALK for the 50 year period. The influence of the changes on ~~the carbonate chemistry~~ (pH and aragonite saturation state ~~changes of about~~ 0.001 and 0.02 respectively), are small compared to the changes predicted from increasing atmospheric CO_2 thereby allowing us to assume that the CARS salinity used has not changed in our calculations.

Sea surface temperature (SST) measurements from 1870 to the present day were obtained from the HadiSST v1.1 dataset (1° × 1°; Rayner et al., 2003). Higher resolution datasets do exist, e.g. NOAA OI V2 (0.25° × 0.25°; Reynolds et al., 2007), but none have estimates beyond the last 3 decades, ~~and~~ we chose the 1° × 1° product to extend our reconstruction back to pre-industrial period.

We first calculated DIC from TALK, SST and $p\text{CO}_2$ in the period 1870–2013, using the method of Lenton et al. (2012) ~~that used~~ the dissociation constants from Mehrbach et al. (1973) refitted by Dickson and Millero (1987). This approach calculates the ~~magnitude of the~~ seasonal cycle of DIC, rather than $p\text{CO}_2$. The $p\text{CO}_2$ seasonality changes over time in response to changes in the Revelle factor and will influence the air–sea gradient in $p\text{CO}_2$, which drives net flux across the air–sea boundary. To correct for this, we first calculated the (detrended) seasonal anomaly of DIC in the period 1995–2006. We then added this seasonal cycle to the deseasonalised long-term DIC record (1870–2013) to reconstruct the DIC fields, thereby allowing $p\text{CO}_2$ to change. The reconstructed DIC fields were then used in conjunction with our derived alkalinity fields to calculate changes in ocean acidification in the period 1870–2013. As the resolution of SST and $p\text{CO}_2$ fields are nominally $1° \times 1°$ monthly fields, all values were calculated on a $1° \times 1°$ grid. The values of pH ~~are~~ calculated using the total scale following recommendations of Riebesell et al. (2010) while aragonite and calcite saturation states were calculated following Mucci (1983).

3 Results and discussion

3.1 Assessment of the mean state and seasonal variability at coastal NRS sites

The ability of our reconstruction to predict the mean state and seasonality of ocean acidification around Australia is evaluated by comparing our calculated aragonite saturation state and SST data with carbonate chemistry and SST measurements made over the last few years from seven of the eight Australian IMOS-NRS sites (Fig. 2; https://imos.aodn.org.au). The Darwin NRS site was not used in the comparison due to the small number of measurements at this site. To assess how well the observed response at the NRS sites were captured, we calculated both the correlation coefficient (R) and the bias (or bias function) (Table 2).

The observed responses from the NRS sites compared with HadiSST are shown in Fig. 3. There is a good correlation in SST at all sites ($r > 0.84$, Table 2) providing confidence that HadiSST represent the character of the seasonal variability. While HadiSST captures the SST variability there were some biases in the mean SST value (Table 2). These biases~~,~~ e.g. Rottnest Island~~,~~ likely reflect local process in the coastal environment at the NRS ~~e.g.~~ Lima and Wethey (2012) that are poorly represented by the much larger spatial scale of the HadiSST product.

The reconstructed aragonite saturation state (Ω_{AR}) show good agreement with values calculated from observations (Fig. 4). The implication is that the salinity–total alkalinity relationship and calculated $p\text{CO}_2$ fields, which are derived mostly from offshore data, are valid for most of the IMOS-NRS sites, which tend to be located on the outer shelf. Exceptions are the Ningaloo and Yongala sites, where our reconstruction overestimates the observed values of aragonite saturation state while SST agrees well with HadiSST (Table 2). The total alkalinity–salinity relationship may not hold at these two sites due to the influence of net calcification ~~on~~ nearby coral reef systems and possibly sediment–water exchange that could alter the total alkalinity ~~e.g.~~ Shaw et al. (2012).

Apart from the offsets at the Yongala and Ningaloo sites, the reconstructed aragonite saturation state do recreate the range determined at most locations (e.g. Maria Island, Port Hacking, Yongala, Rottnest, and North Stradbroke Island). Limited sampling at Kangaroo Island, Esperance and Ningaloo sites prevent direct comparisons of the seasonal variability although the reconstructed variability is ~~plausible based on~~ available measurements.

Overall the ability of our reconstruction to capture the mean state and variability of ocean acidification at the IMOS-NRS sites, gives us confidence in the reconstruction of ocean acidification in the shelf and offshore waters around Australia, and to extend back in time.

3.2 Annual mean state

The mean state of aragonite saturation state around Australia for the period 2000–2009 is shown in Fig. 5. The mean state shows a strong latitudinal gradient in aragonite saturation increasing from values of 1.8 in the southern part of the domain to values greater than 3.9 across Northern Australia and into the Coral Sea. The Coral Sea and Western Pacific form part of the coral triangle, a globally significant region in terms of coral and marine diversity (Bell et al., 2011). We see that our reconstructed values in the Coral Sea and into the Western Pacific are also consistent with the observational values of 3.9 calculated by Kuchinke et al. (2014) in this region. This value is well above 3.5, considered to be a key threshold at which corals move from healthy to marginal conditions (Guinotte et al., 2003).

Ricke et al. (2013), using results from an ensemble of CMIP5 simulations and GLO-DAP data reported that in the Coral Sea, the present-day values of aragonite saturation state are much less than the 3.5 threshold (Guinotte et al., 2003). These differences are explained by the correction of CMIP5 simulations to GLODAP DIC and ALK values (Key et al., 2004) that have very few measurements in this region.

The annual mean state of pH for the period 2000–2009 is shown in Fig. 5. In contrast with aragonite saturation state there is a strong increasing latitudinal gradient from ~ 8.1 in Northern Australia to ~ 8.14 in Southern Australia. The reconstructed values show good agreement on the southern Papua New Guinea coast with Milne Bay observations of Fabricius et al. (2011). However, south of Australia, the pH decreases again to values comparable with those seen in Northern Australia.

The spatial gradients of pH and aragonite saturation state as function of latitude are consistent with the gradients calculated from observations of carbonate chemistry from GLODAP (Key et al., 2004). The distribution of aragonite saturation state is set by both the large-scale distribution of SST, which shows a strong latitudinal gradient, and ALK. Consequently the spatial differences between aragonite saturation state and pH are driven by temperature.

3.3 The seasonal cycle

The seasonal standard deviation (2-sigma) of aragonite saturation state and pH reveal large spatial differences in the magnitude of the seasonal variability (Fig. 5, lower panels). Large seasonality in aragonite saturation state is evident, > 0.4 units. This spatial pattern of this seasonality is quite heterogeneous, with the largest variability occurring along the East Coast of Australia, in the Tasman Sea, and off Southern Australia. The low seasonal variability predicted in the Coral Sea suggests the aragonite saturation state is above 3.5 even in the winter months. Strong and heterogeneous seasonality in pH is also present, > 0.6 units, around Australia, with the largest range off Southern Australia.

The locations of large seasonality in aragonite saturation state and pH off Southern Australia are associated with regions of deep winter mixing > 200 m (Condie and Dunn, 2006). Here, the seasonal deepening of the mixed layer in winter supplies carbon, alkalinity and nutrients to the surface ocean, which in turn alter the chemistry of the surface waters inducing large seasonal variability in ocean acidification values in the surface ocean. The large seasonal variability in aragonite saturation is not associated with large seasonal variability in pH along the East Coast of Australia and in the Tasman Sea, which suggests that the seasonality variability is driven by seasonal changes in SST rather than ocean dynamics. An important consequence of the uncoupling of the pattern of pH and aragonite saturation state is that the biological responses to ocean acidification at the seasonal scale may shift as the susceptibility to pH and aragonite saturation varies between organisms. This has implications for understanding ecosystem responses to ocean acidification.

Small areas of large seasonal variability are also present along parts of the northern of Australia and off Papua New Guinea. These are primarily driven by large seasonal changes in sea surface salinity driving changes in total alkalinity which influences the pH and aragonite saturation state.

3.4 Assessment of annual mean state and seasonality

In this section the reconstructed annual mean and seasonality of pH and aragonite saturation state are compared with that calculated for 2005 (Takahashi et al., 2014); hereafter-denoted T14 (Fig. 6). The data of T14 are based on oceanic pCO$_2$ measurements and regional potential alkalinity vs. salinity relationships, at a resolution of 4° × 5°. Since T14 excludes Equatorial Pacific (north of 8S) data and coastal data, we can only compare our results T14 away from these regions.

The T14 spatial pattern of annual mean of aragonite saturation state appears to be in reasonable agreement with our reconstruction for most waters around Australia. An exception is off Northwestern Australia where the mean aragonite saturation state of T14 appears to be an under-estimate. Large differences in the seasonal changes also occur in off the east coast of Australia and to the South of Australia. The magnitude of the seasonal variability (in T14) is lower than our reconstruction.

The pH values of T14 and our reconstruction both show the highest values in the subtropical waters, although T14 mean values are higher off eastern Australia and lower to the South of Australia. Overall there is quite poor agreement in both the magnitude and spatial pattern of pH variability for most regions.

That the spatial pattern of seasonal cycle of aragonite state is not reproduced along the East Coast of Australia and in the Tasman Sea and the variability in Southern Australia is not seen in either pH nor aragonite saturation state suggested that while the seasonal response of SST is captured in T14, the seasonal ocean dynamics are not well represented. Furthermore the underestimation of the magnitude of the seasonal cycle, particularly in regions in which the pattern of the seasonal cycle is reproduced, likely reflects: (i) the coarser resolution of T14 the product than the reconstruction (4° × 5° vs. 1° × 1°) and the spatial interpolation required to generate T14; and (ii) the T14 relies on a spatial interpolation scheme that may not capture the regional circulation at the scales being considered here.

As result of this analysis we believe that in the Australian region our reconstruction offers an improved and higher resolution representation of the mean state and seasonality than T14. This comparison also underscores the need for such ongoing regional analyses, and the limitations of using large-scale global products such as T14 to understand regional variability and change.

3.5 Historical changes

Historical change in ocean acidification since 1870 is represented in Fig. 7 by the changes in the mean annual values of pH and aragonite saturation state between the period 1870–1889 and 1990–2009 (Fig. 7). The corresponding changes in sea surface temperature (HadiSST; Rayner et al., 2003) are shown over the same period, indicating a small net warming of the waters around Australia. This warming has been relatively uniform with the exception of the northern edge of the Southern Ocean, and Southeastern Australia which is identified as a marine hotspot by Hobday and Pecl (2013). The ocean acidification changes due to ocean carbon uptake driven by increasing atmospheric CO$_2$, rather than changes in SST. The changes with time in pH and saturation state at the IMOS-NRS sites are plotted in Fig. 8.

Our reconstruction shows the oceanic carbon uptake over the last 120 years has resulted in decrease in aragonite saturation state of 0.48. As illustrated in Fig. 8 these decreases are not constant with time and the change in aragonite saturation state is accelerating. There is also a strong latitudinal gradient in magnitude of the decrease, with larger changes occurring in Northern Australian waters and smaller changes to the south. However the largest decreases in in aragonite saturation state (< 0.6) have occurred in the Tasman Sea and along the southern coast of Australia. These large changes are illustrated at the NRS sites Port Hacking, Ningaloo and Kangaroo Island (Fig. 10). This pattern of change around Australia is consistent with large-scale chemical buffering capacity of the ocean (Revelle factor) e.g. (Sabine et al., 2004).

Consistent with aragonite saturation state over the last 120 years there has been a net decease in pH of 0.09 units, very close to the estimated global decrease of 0.1

pH by (Caldeira and Wickett, 2003) ~~over a similar period~~. Consistent with aragonite saturation a strong latitudinal gradient in pH is evident~~, but it is the inverse~~. The largest changes in pH have occurred in Southern Australia ~~e.g.~~ Maria Island (Fig. 8), with the smallest changes in Northern Australian waters (~~e.g.~~ Yongala ~~(Fig. 8)~~ is about 75 % of the change experienced in the south). <mark>This spatial response of pH is primarily set by the gradient of ocean mean temperature that acts to increase pH in colder waters.</mark>

3.6 Interannual variability

~~Our reconstruction reconstructs the magnitude of interannual variability around Australia (Fig. 7) in pH and aragonite saturation state over the period 1870–2013.~~ The magnitude of the interannual variability at the 2-σ level was also calculated after the long-term trend ~~in aragonite saturation state and pH~~ were removed using a 20 year running mean filter (Fig. 8).

The magnitude of the interannual variability in aragonite saturation state from the reconstruction is small (0.05 domain averaged; 2-σ) and spatially homogenous. With the largest interannual variability in aragonite saturation state occurring in the far eastern Tasman Sea associated with the largest interannual variability in SST. In contrast the smallest variability is seen along the boundary of the Southern Ocean where SST interannual variability is least. Consistent with aragonite saturation state the pH interannual variability is small (0.002 domain averaged; 2-σ) around Australia. While there appears to be more spatial heterogeneity in the response of pH, the magnitude is very small. Nevertheless, we do see areas of concomitant variability in pH and aragonite saturation state suggesting that in these regions there is interannual variability in the supply of carbon and nutrients to the surface ocean, which ~~in turn would alter~~ the chemistry of the surface waters ~~rather than~~ SST changes ~~alone~~.

To put the interannual variability in aragonite saturation state and pH in context we calculate the ratio of seasonal variability to interannual variability in Fig. 9. The dominant scale of variability is seasonal for both aragonite saturation state and pH, ~~however there is a~~ distinct spatial pattern to this ratio (Fig. 9). For aragonite saturation state,

8277

the seasonal variability is larger than interannual variability in the South, while the ratio of seasonal variability is much closer to the magnitude of interannual variability in the Coral Sea. This means that observationally separating seasonal changes from interannual changes will be challenging, and may have implications for interpreting observational records. By contrast, around most of Australia the seasonal variability in pH dominates interannual variability with the exception of the Tasman Sea and is much larger than ~~the ratio~~ for aragonite saturation state. In the Tasman Sea, the magnitude of the seasonal variability is close to unity suggesting that in this region it would again be difficult to separate seasonal changes from interannual changes.

3.7 Robustness of the reconstruction

The interannual variability and trend in aragonite saturation state and pH in ~~the~~ reconstruction ~~as presented~~ are driven wholly by SST and atmospheric CO_2, and thereby neglects any changes in interannual variability due changes in salinity and biological production. Observationally, studies have suggested that in some regions around Australia changes in salinity over the last 50 years have occurred e.g. Durack and Wijffels (2010), while other regions have remained constant over the last 200 years e.g. Calvo et al. (2007). If we assume, consistent with (Durack et al., 2012), that the changes are related to evaporation–precipitation (E–P) rather than local riverine input which can have large local inputs of DIC, ALK and potentially nutrients (Hieronymus and Walin, 2013), then any increase in salinity can be treated as freshwater input only. Consequently given the small trends, relative to the mean, and the very low sensitivity of oceanic $p\mathrm{CO}_2$ to freshwater input ($< 1\,\%$), it is highly unlikely that such changes would make such a significant difference on pH or aragonite over the last 50 years. This is perhaps not surprising given that freshwater water changes are a dilution flux acting equally on DIC and total alkalinity (Lenton et al., 2012).

The nutrients ~~driving~~ variability in ocean acidification are also not considered in this study, as we assume that nutrients are zero around Australia. While this is not strictly true, most waters around Australia are oligotrophic in nature (Condie and Dunn, 2006).

8278

If the climatological values of silicate and nitrate from CARS (Ridgway et al., 2002) are used to calculate carbonate chemistry, we find only a small bias (0.0007 in aragonite saturation state and 0.005 in pH) in our reconstruction. While we would like to have used a time-evolving field, analogous to salinity, at present no long-term time series are available ~~to use in this reconstruction~~.

In this study we also assume that the seasonal air–sea disequilibrium ($\Delta p\text{CO}_2$) is time invariant i.e. no interannual variability. This is clearly not the case as values of oceanic $p\text{CO}_2$ can be impacted by changes in SST and biological production. While the changes in SST are accounted for in carbonate chemistry, they are not accounted for oceanic $p\text{CO}_2$. This suggests that interannual variability is likely to be underestimated in this study. Recent studies have reconstructed time-evolving $\Delta p\text{CO}_2$ fields e.g. (Landschützer et al., 2014) these products typically only extend back in time several decades as they are based on an interpolation of ocean observations and atmospheric CO_2 records, thereby only allowing reconstructing of ocean acidification over several decades. If we account for this interannual variability, the ratio of seasonal variability to interannual variability is likely to decrease (Fig. 9). ~~This suggests that~~ separating seasonal and interannual variability will be complicated for regions with a low ratio for aragonite saturation state (i.e. the Coral Sea and Tropical Ocean) and for pH (i.e. Tasman Sea), which has potential implications for interpreting observed biological changes.

In the case of biological production as primary production is very low around much of Australia (Condie and Dunn, 2006) ($< 0.2\,\text{mg}\,\text{m}^{-3}$) it is unlikely that even a doubling of primary productivity in response to interannual changes in nutrient supply could induce large changes oceanic $p\text{CO}_2$ around Australia. Consequently it is unlikely that variability in primary production likely plays a large role in modulating interannual variability. The exception to this is along the boundary of the Southern Ocean in the SubAntarctic Zone where large changes in biological production have been observed (Mongin et al., 2011).

4 Conclusions

To explore how Australia's marine environment has changed, we have synthesised newly acquired in situ observations of carbon chemistry around Australia to: (i) provide an new estimate of the mean state of pH and aragonite saturation state, (ii) estimate seasonal and interannual variability since 1870; and (iii) reconstruct the changes in ocean acidification around Australia since 1870.

In this work we developed a new alkalinity–salinity relationship for the Australian region. This relationship was used in conjunction with observed salinity and oceanic and atmospheric CO_2 and SST data, to reconstruct the present and past changes in pH and aragonite saturation state. Our reconstructed fields were compared against another climatology and high-resolution data collected at the IMOS-NRS sites. We found good agreement between our reconstructed fields for the observed annual mean and seasonal cycles at the shelf IMOS-NRS sites except regions such as the Great Barrier Reef where nearshore processes and coral reef metabolism could alter the pH and saturation state.

Our regional reconstruction provides much higher spatial and temporal resolution than previous global estimates. ~~This highlights the importance of regional analysis and reconstructions in estimating and understanding region changes.~~ An important result of this study is that at present the Coral Sea is not experiencing marginal conditions with respect to ocean acidification as has been suggested.

Large changes in aragonite saturation state and pH have occurred over the last 140 years in response to increasing oceanic uptake of atmospheric CO_2. A net decrease of in pH of 0.09 is seen in the period 1990–2009–1889–1870, together with a net decrease in aragonite saturation state of 0.48, both of which are consistent with previous estimates of the historical trends. Importantly, due to ocean chemistry, the spatial pattern of the change in aragonite saturation state and pH are different. In this study we found the largest changes in aragonite saturation state occurred at mid and low latitudes, and the largest changes in pH occurred at higher latitudes.

The large seasonal variability around Australia is heterogeneous, with distinctly different spatial patterns in aragonite saturation state and pH apart from South of Australia where variability is driven by deep winter mixing. For aragonite saturation state, large seasonal variability occurs off the East Coast of Australia and in Tasman Sea driven by seasonal variability in ocean temperatures. Generally, the magnitude of seasonal variability exceeds IAV in the Australian region with the exception of pH in Tasman Sea, and aragonite saturation state in the tropical ocean. In these regions the magnitude of interannual variability is comparable to seasonal variability, which has potential implications for interpreting observed biological changes at over different timescales.

The variability in aragonite saturation state and pH are spatially different over regional scales and all time scales, implying that biological responses and impacts are likely vary. Further, this suggests that both pH and aragonite (or calcite) saturation state need to be considered independently in assessing ecosystem responses and changes.

The goal of this historical reconstruction also provides useful information to link with biological observations to help understand observed changes and aid in the design of future work, thereby elucidating the consequences of Ocean Acidification. To facilitate this all of the reconstructed data is available at http://imos.aodn.org.au.

References

Albright, R., Langdon, C., and Anthony, K. R. N.: Dynamics of seawater carbonate chemistry, production, and calcification of a coral reef flat, central Great Barrier Reef, Biogeosciences, 10, 6747–6758, doi:10.5194/bg-10-6747-2013, 2013.

Bell, J. D., Johnson, J. E, and Hobday, A. J. (Eds.): Vulnerability of Tropical Pacific Fisheries and Aquaculture to Climate Change, Secretariat of the Pacific Community, Noumea, New Caledonia, 2011.

Caldeira, K. and Wickett, M. E.: Anthropogenic carbon and ocean pH, Nature, 425, 365–365, doi:10.1038/425365a, 2003.

Calvo, E., Marshall, J. F., Pelejero, C., McCulloch, M. T., Gagan, M. K., and Lough, J. M.: Interdecadal climate variability in the Coral Sea since 1708 AD, Palaeogeogr. Palaeocl., 248, 190–201, doi:10.1016/J.Palaeo.2006.12.003, 2007.

Ciais, P., Sabine, C., Bala, G., Bopp, L., Brovkin, V., Canadell, J., Chhabra, A., DeFries, R., Galloway, J., Heimann, M., Jones, C., Le Quéré, C., Myneni, R. B., Piao, S. and Thornton, P.: Carbon and Other Biogeochemical Cycles, in: Climate Change 2013: The Physical Science Basis, Contribution of Working Group I to the Fifth Assessment Report of the Intergovernmental Panel on Climate Change, edited by: Stocker, T. F., Qin, D., Plattner, G.-K., Tignor, M., Allen, S. K., Boschung, J., Nauels, A., Xia, Y., Bex, V., and Midgley, P. M., Cambridge University Press, Cambridge, United Kingdom and New York, NY, USA, 465–570, doi:10.1017/CBO9781107415324.015, 2013.

Condie, S. A. and Dunn, J. R.: Seasonal characteristics of the surface mixed layer in the Australasian region: implications for primary production regimes and biogeography, Mar. Freshwater. Res., 57, 569–590, doi:10.1071/MF06009, 2006.

Dickson, A. G. and Millero, F. J.: A comparison of the equilibrium constants for the dissociation of carbonic acid in seawater media, Deep-Sea Res. Pt. I, 34, 1733–1743, doi:10.1016/0198-0149(87)90021-5, 1987

Doney, S. C., Balch, W. M., Fabry, V. J., and Feely, R. A.: Ocean acidification: a critical emerging problem for the ocean sciences, Oceanography, 22, 16–25, doi:10.5670/Oceanog.2009.93, 2009.

Doney, S. C., Ruckelshaus, M., Duffy, J. E., Barry, J. P., Chan, F., English, C. A., Galindo, H. M., Grebmeier, J. M., Hollowed, A. B., Knowlton, N., Polovina, J., Rabalais, N. N., Sydeman, W. J., and Talley, L. D.: Climate change impacts on marine ecosystems, Annu. Rev. Mar. Sci., 4, 11–37, doi:10.1146/Annurev-Marine-041911-111611, 2012.

Dore, J. E., Lukas, R., Sadler, D. W., Church, M. J., and Karl, D. M.: Physical and biogeochemical modulation of ocean acidification in the central North Pacific, P. Natl. Acad. Sci. USA, 106, 12235–12240, doi:10.1073/Pnas.0906044106, 2009.

Durack, P. J. and Wijffels, S. E.: Fifty-year trends in global ocean salinities and their relationship to broad-scale warming, J. Climate, 23, 4342–4362, doi:10.1175/2010jcli3377.1, 2010.

Durack, P. J., Wijffels, S. E., and Matear, R. J.: Ocean salinities reveal strong global water cycle intensification during 1950 to 2000, Science, 336, 455–458, doi:10.1126/Science.1212222, 2012.

Fabricius, K. E., Langdon, C., Uthicke, S., Humphrey, C., Noonan, S., De'ath, G., Okazaki, R., Muehllehner, N., Glas, M. S., and Lough, J. M.: Losers and winners in coral reefs acclimatized to elevated carbon dioxide concentrations, Nature Climate Change, 1, 165–169, doi:10.1038/Nclimate1122, 2011.

Fabry, V. J., Seibel, B. A., Feely, R. A., and Orr, J. C.: Impacts of ocean acidification on marine fauna and ecosystem processes, Ices J. Mar. Sci., 65, 414–432, doi:10.1093/Icesjms/Fsn048, 2008.

Frolicher, T. L. and Joos, F.: Reversible and irreversible impacts of greenhouse gas emissions in multi-century projections with the NCAR global coupled carbon cycle-climate model, Clim. Dynam., 35, 1439–1459, doi:10.1007/S00382-009-0727-0, 2010.

Gagliano, M., McCormick, M. I., Moore, J. A., and Depczynski, M.: The basics of acidification: baseline variability of pH on Australian coral reefs, Mar. Biol., 157, 1849–1856, doi:10.1007/S00227-010-1456-Y, 2010.

Guinotte, J. M., Buddemeier, R. W., and Kleypas, J. A.: Future coral reef habitat marginality: temporal and spatial effects of climate change in the Pacific basin, Coral. Reefs., 22, 551–558, doi:10.1007/S00338-003-0331-4, 2003.

Hieronymus, J. and Walin, G.: Unravelling the land source: an investigation of the processes contributing to the oceanic input of DIC and alkalinity, Tellus B, 65, 19683, doi:10.3402/Tellusb.V65i0.19683, 2013.

Hobday, A. J. and Pecl, G. T.: Identification of global marine hotspots: sentinels for change and vanguards for adaptation action, Rev. Fish. Biol. Fisher., 24, 415–425, doi:10.1007/s11160-013-9326-6, 2013.

Iglesias-Rodriguez, M. D., Halloran, P. R., Rickaby, R. E. M., Hall, I. R., Colmenero-Hidalgo, E., Gittins, J. R., Green, D. R. H., Tyrrell, T., Gibbs, S. J., von Dassow, P., Rehm, E., Armbrust, E. V., and Boessenkool, K. P.: Phytoplankton calcification in a high-CO_2 world, Science, 320, 336–340, doi:10.1126/Science.1154122, 2008.

Key, R. M., Kozyr, A., Sabine, C. L., Lee, K., Wanninkhof, R., Bullister, J. L., Feely, R. A., Millero, F. J., Mordy, C., and Peng, T. H.: A global ocean carbon climatology: results

from Global Data Analysis Project (GLODAP), Global Biogeochem. Cy., 18, Gb4031, doi:10.1029/2004gb002247, 2004.

Kuchinke, M., Tilbrook, B., and Lenton, A.: Seasonal variability of aragonite saturation state in the Western Pacific, Mar. Chem., 161, 1–13, doi:10.1016/J.Marchem.2014.01.001, 2014.

Langdon, C. and Atkinson, M. J.: Effect of elevated pCO2 on photosynthesis and calcification of corals and interactions with seasonal change in temperature/irradiance and nutrient enrichment, J. Geophys. Res., 110, C09207, doi:10.1029/2004jc002576, 2005.

Le Quéré, C., Moriarty, R., Andrew, R. M., Peters, G. P., Ciais, P., Friedlingstein, P., Jones, S. D., Sitch, S., Tans, P., Arneth, A., Boden, T. A., Bopp, L., Bozec, Y., Canadell, J. G., Chini, L. P., Chevallier, F., Cosca, C. E., Harris, I., Hoppema, M., Houghton, R. A., House, J. I., Jain, A. K., Johannessen, T., Kato, E., Keeling, R. F., Kitidis, V., Klein Goldewijk, K., Koven, C., Landa, C. S., Landschützer, P., Lenton, A., Lima, I. D., Marland, G., Mathis, J. T., Metzl, N., Nojiri, Y., Olsen, A., Ono, T., Peng, S., Peters, W., Pfeil, B., Poulter, B., Raupach, M. R., Regnier, P., Rödenbeck, C., Saito, S., Salisbury, J. E., Schuster, U., Schwinger, J., Séférian, R., Segschneider, J., Steinhoff, T., Stocker, B. D., Sutton, A. J., Takahashi, T., Tilbrook, B., van der Werf, G. R., Viovy, N., Wang, Y.-P., Wanninkhof, R., Wiltshire, A., and Zeng, N.: Global carbon budget 2014, Earth Syst. Sci. Data, 7, 47–85, doi:10.5194/essd-7-47-2015, 2015.

Lee, K., Tong, L. T., Millero, F. J., Sabine, C. L., Dickson, A. G., Goyet, C., Park, G. H., Wanninkhof, R., Feely, R. A., and Key, R. M.: Global relationships of total alkalinity with salinity and temperature in surface waters of the world's oceans, Geophys. Res. Lett., 33, L19605, doi:10.1029/2006gl027207, 2006.

Lenton, A., Metzl, N., Takahashi, T., Kuchinke, M., Matear, R. J., Roy, T., Sutherland, S. C., Sweeney, C., and Tilbrook, B.: The observed evolution of oceanic pCO(2) and its drivers over the last two decades, Global Biogeochem. Cy., 26, Gb2021, doi:10.1029/2011gb004095, 2012.

Lima, F. P. and Wethey, D. S.: Three decades of high-resolution coastal sea surface temperatures reveal more than warming, Nat. Commun., 3, 704, doi:10.1038/Ncomms1713, 2012.

Lynch, T. P., Morello, E. B., Evans, K., Richardson, A., Rochester, J. W. C., Steinberg, C. R., Roughan, M., Thompson, P., Middleton, J. F., Feng, M., Sherrington, R., Brando, V., Tilbrook, B., Ridgway, K., Allen, S., Doherty, P., Hill, K., and Moltmann, T. C.: IMOS national reference stations: a continental wide physical, chemical and biological coastal observing system, PLOS One, 9, e113652, doi:10.1371/journal.pone.0113652, 2014.

Matear, R. J. and Lenton, A.: Quantifying the impact of ocean acidification on our future climate, Biogeosciences, 11, 3965–3983, doi:10.5194/bg-11-3965-2014, 2014.

Mehrbach, C., Culberson, C. H., Hawley, J. E., and Pytkowicz, R. M.: Measurement of the apparent dissociation constants of carbonic acid in seawater at atmospheric pressure, Limnol. Oceanogr., 18, 897–907, doi:10.4319/lo.1973.18.6.0897, 1973.

Mongin, M., Matear, R., and Chamberlain, M.: Seasonal and spatial variability of remotely sensed chlorophyll and physical fields in the SAZ-Sense region, Deep-Sea Res. Pt. II, 58, 2082–2093, doi:10.1016/J.Dsr2.2011.06.002, 2011.

Mucci, A.: The solubility of calcite and aragonite in seawater at various salinities, temperatures, and one atmosphere total pressure, Am. J. Sci., 283, 780–799, 1983.

Munday, P. L., Donelson, J. M., Dixson, D. L., and Endo, G. G. K.: Effects of ocean acidification on the early life history of a tropical marine fish, P. Roy. Soc. B-Biol. Sci., 276, 3275–3283, doi:10.1098/Rspb.2009.0784, 2009.

Munday, P. L., Dixson, D. L., McCormick, M. I., Meekan, M., Ferrari, M. C. O., and Chivers, D. P.: Replenishment of fish populations is threatened by ocean acidification, P. Natl. Acad. Sci. USA, 107, 12930–12934, doi:10.1073/Pnas.1004519107, 2010.

Pelejero, C., Calvo, E., McCulloch, M. T., Marshall, J. F., Gagan, M. K., Lough, J. M., and Opdyke, B. N.: Preindustrial to modern interdecadal variability in coral reef pH, Science, 309, 2204–2207, doi:10.1126/Science.1113692, 2005.

Rayner, N. A., Parker, D. E., Horton, E. B., Folland, C. K., Alexander, L. V., Rowell, D. P., Kent, E. C., and Kaplan, A.: Global analyses of sea surface temperature, sea ice, and night marine air temperature since the late nineteenth century, J. Geophys. Res.-Atmos., 108, 4407, doi:10.1029/2002jd002670, 2003.

Reynolds, R. W., Smith, T. M., Liu, C., Chelton, D. B., Casey, K. S., and Schlax, M. G.: Daily high-resolution-blended analyses for sea surface temperature, J. Climate, 20, 5473–5496, doi:10.1175/2007jcli1824.1, 2007.

Ricke, K. L., Orr, J. C., Schneider, K., and Caldeira, K.: Risks to coral reefs from ocean carbonate chemistry changes in recent earth system model projections, Environ. Res. Lett., 8, 034003, doi:10.1088/1748-9326/8/3/034003, 2013.

Ridgway, K. R., Dunn, J. R., and Wilkin, J. L.: Ocean interpolation by four-dimensional weighted least squares – application to the waters around Australasia, J. Atmos. Ocean. Tech., 19, 1357–1375, doi:10.1175/1520-0426(2002)019<1357:OIBFDW>2.0.CO;2, 2002.

Riebesell, U., Fabry, V. J., Hansson, L., and Gattuso, J.-P.: Guide to Best Practices for Ocean Acidification Research and Data Reporting, Publications Office of the European Union, Luxembourg, 260 pp., 2010.

Sabine, C. L., Feely, R. A., Gruber, N., Key, R. M., Lee, K., Bullister, J. L., Wanninkhof, R., Wong, C. S., Wallace, D. W. R., Tilbrook, B., Millero, F. J., Peng, T. H., Kozyr, A., Ono, T., and Rios, A. F.: The oceanic sink for anthropogenic CO_2, Science, 305, 367–371, doi:10.1126/Science.1097403, 2004.

Sasse, T. P., McNeil, B. I., and Abramowitz, G.: A new constraint on global air–sea CO_2 fluxes using bottle carbon data, Geophys. Res. Lett., 40, 1594–1599, doi:10.1002/Grl.50342, 2013.

Shaw, E. C., McNeil, B. I., and Tilbrook, B.: Impacts of ocean acidification in naturally variable coral reef flat ecosystems, J. Geophys. Res.-Oceans, 117, C03038, doi:10.1029/2011jc007655, 2012.

Silverman, J., Lazar, B., Cao, L., Caldeira, K., and Erez, J.: Coral reefs may start dissolving when atmospheric CO_2 doubles, Geophys. Res. Lett., 36, L05606, doi:10.1029/2008gl036282, 2009.

Stanley, S. M. and Hardie, L. A.: Secular oscillations in the carbonate mineralogy of reef-building and sediment-producing organisms driven by tectonically forced shifts in seawater chemistry, Palaeogeogr. Palaeocl., 144, 3–19, doi:10.1016/S0031-0182(98)00109-6, 1998.

Takahashi, T., Sutherland, S. C., Wanninkhof, R., Sweeney, C., Feely, R. A., Chipman, D. W., Hales, B., Friederich, G., Chavez, F., Sabine, C., Watson, A., Bakker, D. C. E., Schuster, U., Metzl, N., Yoshikawa-Inoue, H., Ishii, M., Midorikawa, T., Nojiri, Y., Kortzinger, A., Steinhoff, T., Hoppema, M., Olafsson, J., Arnarson, T. S., Tilbrook, B., Johannessen, T., Olsen, A., Bellerby, R., Wong, C. S., Delille, B., Bates, N. R., and de Baar, H. J. W.: Climatological mean and decadal change in surface ocean pCO(2), and net sea–air CO_2 flux over the global oceans, Deep-Sea Res. Pt. II, 56, 554–577, doi:10.1016/J.Dsr2.2008.12.009, 2009.

Takahashi, T., Sutherland, S. C., Chipman, D. W., Goddard, J. G., Ho, C., Newberger, T., Sweeney, C., and Munro, D. R.: Climatological distributions of pH, pCO$_2$, total CO_2, alkalinity, and $CaCO_3$ saturation in the global surface ocean, and temporal changes at selected locations, Mar. Chem., 164, 95–125, doi:10.1016/j.marchem.2014.06.004, 2014.

Table 1. Data used to derive the salinity vs. total alkalinity relationship for surface waters (depth < 40 m) in Australian regional seas.

Voyage/Station	Region	Latitude	Longitude	Time Period	Sample number
TF5[1]	Tasman Sea Coral Sea	9.7–40.3° S	144.5–172.0° E	Feb 2007–Sep 2011	1465
FR[2]	Indian Ocean, CO_2/CLIVAR section	8.0–34.0° S	95.0–114.8° E	Sep 2000–Nov 2000	70
SS[3]	Indian Ocean shelf and offshore waters	20.6–23.0° S	112.8–115.2° E	May 2010	70
NIN[4]	Ningaloo shelf, IMOS reference station	21.9° S	113.9° E	Feb 2011–Aug 2012	20
KAI[4]	Kangaroo Island shelf, IMOS reference station	35.8° S	136.4° E	Oct 2008–Apr 2012	75
Total					1700

[1] http://cdiac.ornl.gov/ftp/oceans/VOS_TF5_Line/,
[2] http://cdiac.ornl.gov/ftp/oceans/CLIVAR/I02_2000.data/,
[3] http://www.marine.csiro.au/marq/edd_search.Browse_Citation?txtSession=8681,
[4] http://imos.aodn.org.au/.

8287

Table 2. The locations of the NRS sites used in this study, along with the biases, correlation coefficent (R) between the SST and aragonite saturation state observed at the site with values from our reconstruction, HadiSST and calculated omega, respectively. Also listed are the number of observations used in calculating the Biases and Correlations.

|	Lat	Lon	SST-BIAS	SST-R	OmA-BIAS	OmA-R	n
Esperance	33°56 S	121°51 E	0.8	0.93	0.09	−0.06	16
Kangaroo Island	35°49 S	136°27 E	0.38	0.84	0.01	0.03	27
Maria Is	42°36 S	148°14 E	0.6	0.93	0.07	0.83	40
Rottnest Is	32°25 S	115°25 E	1.01	0.92	0.06	0.26	33
Ningaloo	21°52 S	113°57 E	0.08	0.95	0.17	0.62	11
Yongala	19°19 S	147°27 E	0.13	0.94	0.27	0.45	37
Port Hacking	34°5 S	151°6 E	0.82	0.89	0.09	0.58	46
North Stradbroke Is	27°18 S	153°6 E	0.08	0.96	0.06	0.78	40

8288
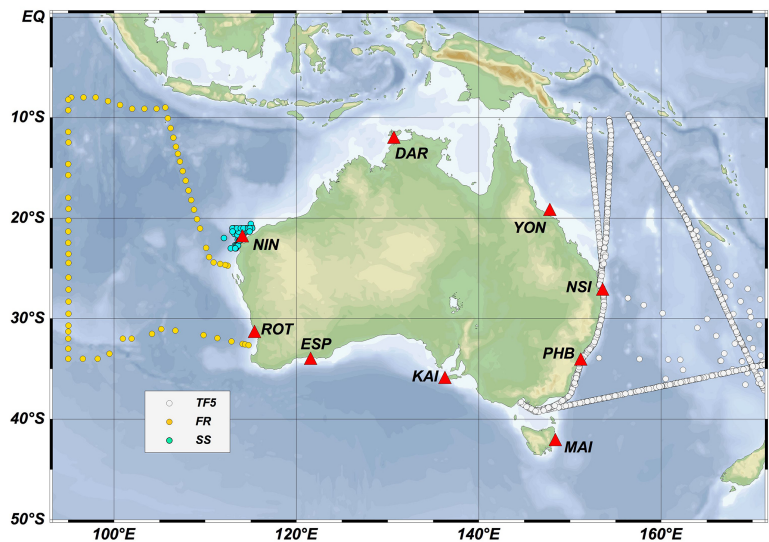
Figure 1. Locations (circles) of the concomitant measurements of alkalinity and salinity used to develop a new salinity–alkalinity relationship for the Australian Region. Overlain on this plot (red triangles) are the locations of IMOS National Reference Stations (NRS). In developing a new salinity–alkalinity relationship only NRS measurements from Ningaloo Reef (NIN) and Kangaroo Island (KIA) were in conjunction with cruise data Transfuture 5 (TF5), the RV *Southern* Surveyor (SS) and the RV *Franklin* (FR). The remaining NRS sites shown are: PHB – Port Hacking; MAI – Maria Island; ESP – Esperance; ROT – Rottnest Island; YON – Yongala, PHB – Port Hacking, NSI – North Stradbroke Island.
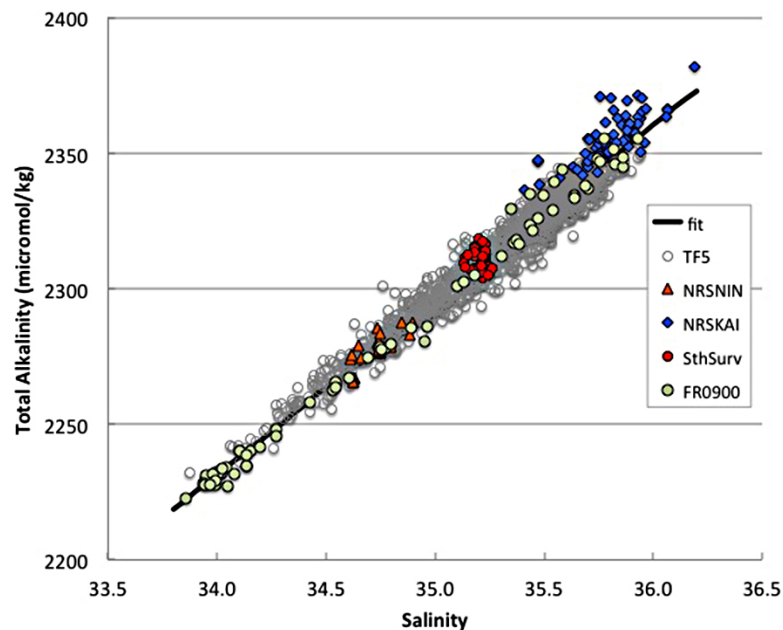
Figure 2. The new salinity–alkalinity relationship developed for the Australian Region based on observations (Fig. 1) collected in the period 2007–2012.
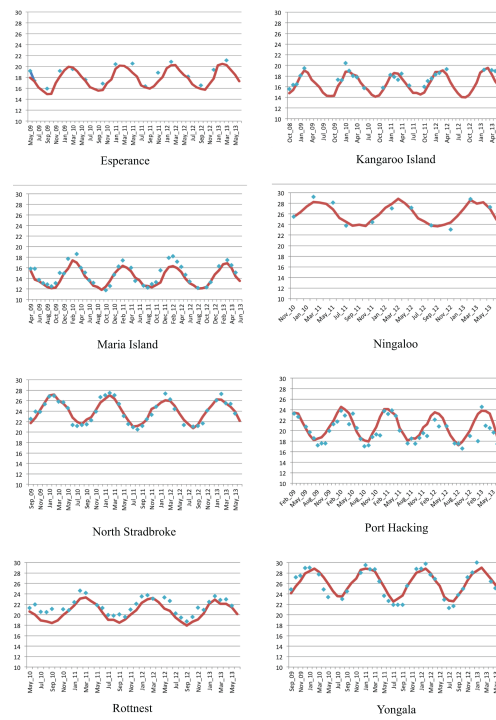
Figure 3. Comparison of sea surface temperature from the observations at the IMOS National Research Stations with HadiSST (Rayner et al., 2003).

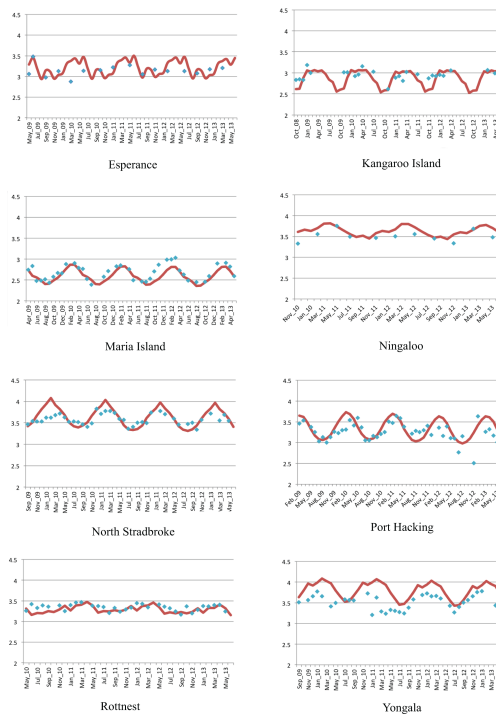**Figure 4.** Comparison of aragonite saturation state (Ω_{AR}) from the observations at the IMOS National Research Stations with the reconstructed values.
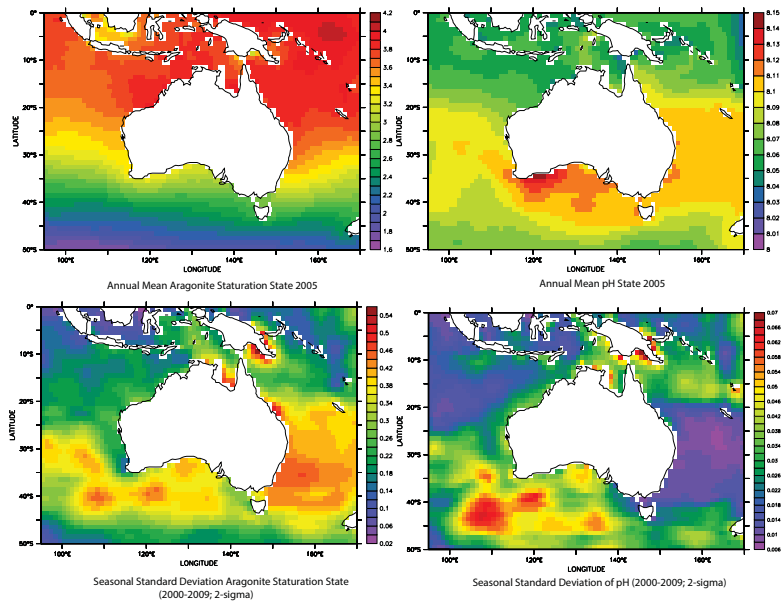
Figure 5. Upper: the reconstructed annual mean aragonite saturation state and pH for the period 2000–2009; lower: the seasonal variability given by 2 times the standard deviation (2-σ) of the seasonal variability in aragonite saturation state and pH from the period 2000–2009.
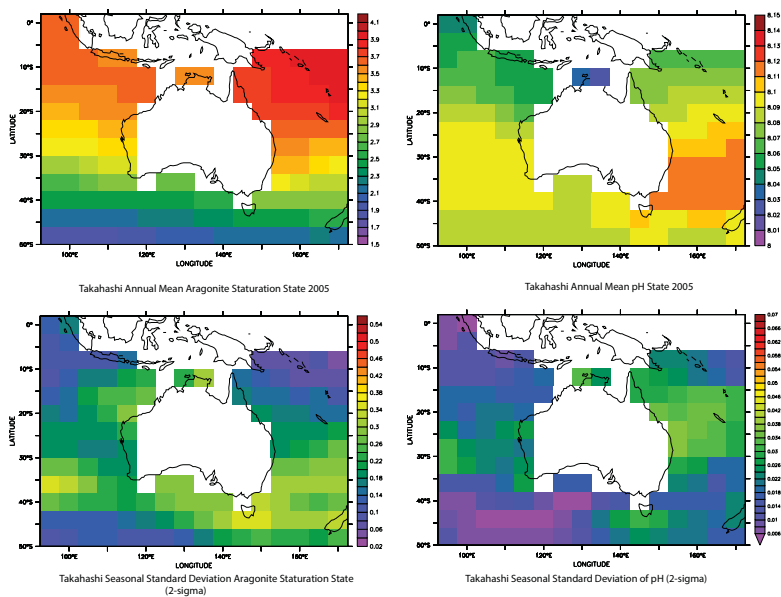
8293

Figure 6. Upper: the annual mean aragonite saturation state and pH for 2005 from Takahashi et al. (2014); lower: standard deviation (2σ) of the seasonal variability in aragonite saturation state and pH for 2005 from Takahashi et al. (2014).
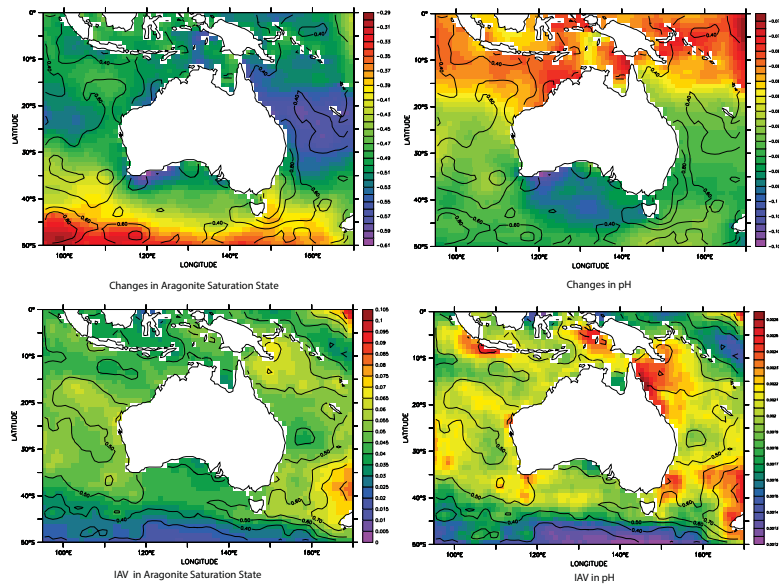
8294

Figure 7. Annual mean 120 year differences (2000–2009 and 1880–1889) in aragonite saturation state and pH (upper) overlain on these plots are the changes in SST over the same period from HadiSST (Rayner et al., 2003); lower, the interannual variability (IAV) in aragonite saturation state and pH (2-σ) over same period, overlain on this plot is the IAV of SST (2-σ) from HadiSST.

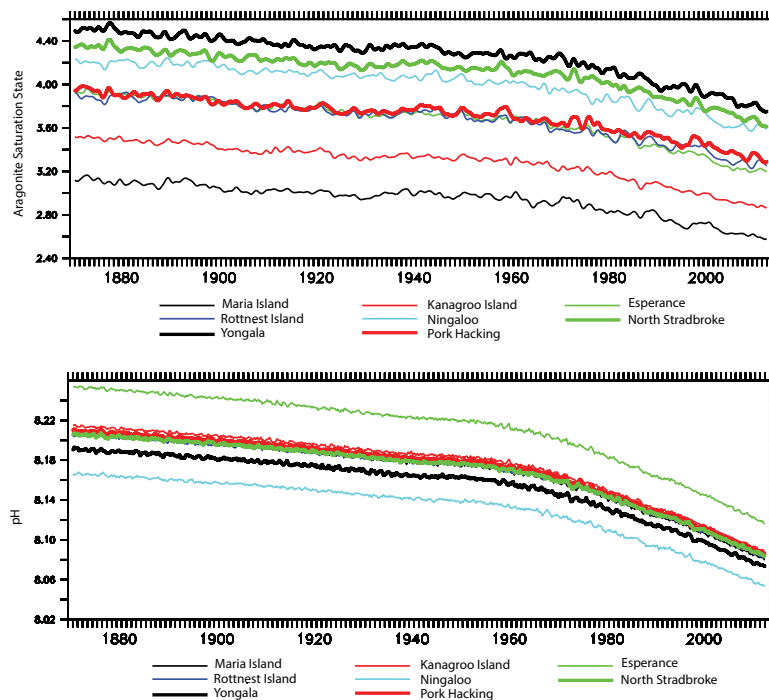**Figure 8.** Reconstructed time series of annual mean aragonite saturation state (upper) and pH (lower) at the IMOS-NRSs.

Seasonal/Interannual Variability in Aragonite Saturation State

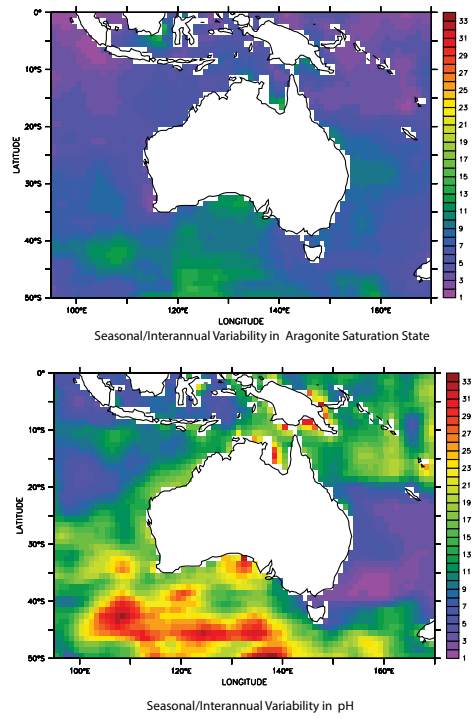Seasonal/Interannual Variability in pH

Figure 9. The ratio of seasonal variability to interannual variability for aragonite saturation state (upper) and pH (lower).